

# MoMuCAMS: A new modular platform for boundary layer aerosol and trace gas vertical measurements in extreme environments

Roman Pohorsky<sup>1</sup>, Andrea Baccarini<sup>1,2</sup>, Julie Tolu<sup>3,4</sup>, Lenny H.E. Winkel<sup>3,4</sup>, Julia Schmale<sup>1</sup>

<sup>1</sup>Extreme Environments Research Laboratory, Ecole Polytechnique Fédérale de Lausanne, Sion, 1950, Switzerland

<sup>2</sup>Now at: Laboratory for Atmospheric Processes and their Impact, Ecole Polytechnique Fédérale de Lausanne, Lausanne, 1015, Switzerland

<sup>3</sup>Eawag, Swiss Federal Institute of Aquatic Science and Technology, Department of Water Resources and Drinking Water (W+T), Dübendorf, 8600, Switzerland

<sup>4</sup>ETH Zurich, Swiss Federal Institute of Technology, Department of Environment Systems Sciences (D-USYS), Institute of Biogeochemistry and Pollutant Dynamics (IBP), Group of Inorganic Environmental Geochemistry, Universitätstrasse 16, 8092 Zurich, Switzerland

Correspondance to: Roman Pohorsky (roman.pohorsky@epfl.ch) and Julia Schmale (julia.schmale@epfl.ch)

## S.1 aMCPC cross-comparison and $d_{50}$ cutoff characterization

Two aMCPCs (aMCPC model 9403, Brechtel Manufacturing Inc) have been compared against a reference MCPC (MCPC model 1720, Brechtel Manufacturing Inc) with PSLs of  $D_p$  150 nm. PSLs were nebulized and dried through a silica gel column. The two aMCPCs and the reference MCPC were connected in parallel behind the drier. Figure S1 shows a scatterplot of 5 minute averaged data for different number concentrations. Both aMCPCs agree well with the reference MCPC. Linear regressions indicate slopes of 0.97 and 1.02 for aMCPC021 and 022, respectively.

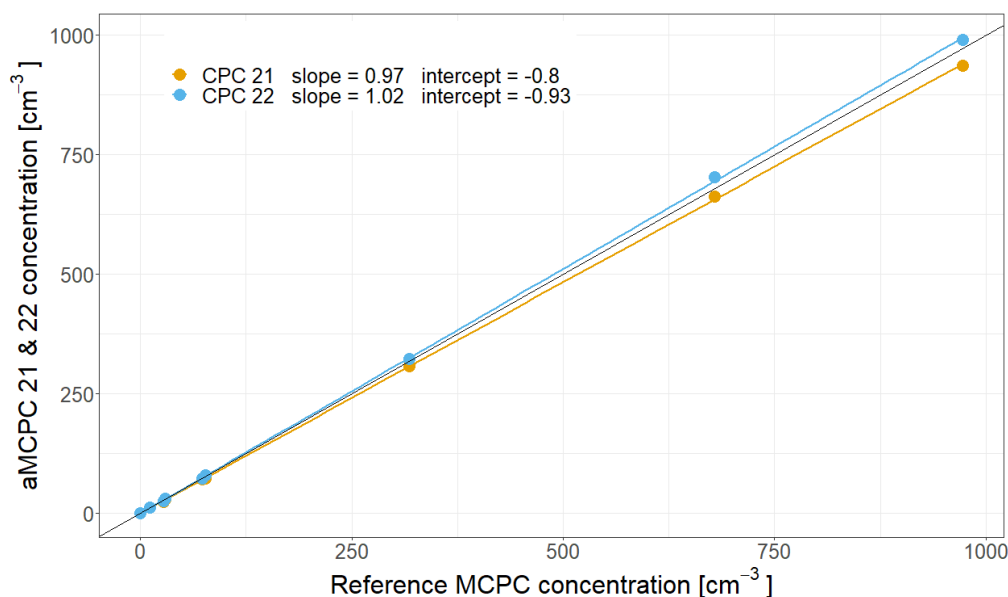


Figure S1: Comparison of two aMCPCs (model 9403, Brechtel Manufacturing Inc) against a reference MCPC (model 1720, Brechtel Manufacturing Inc).

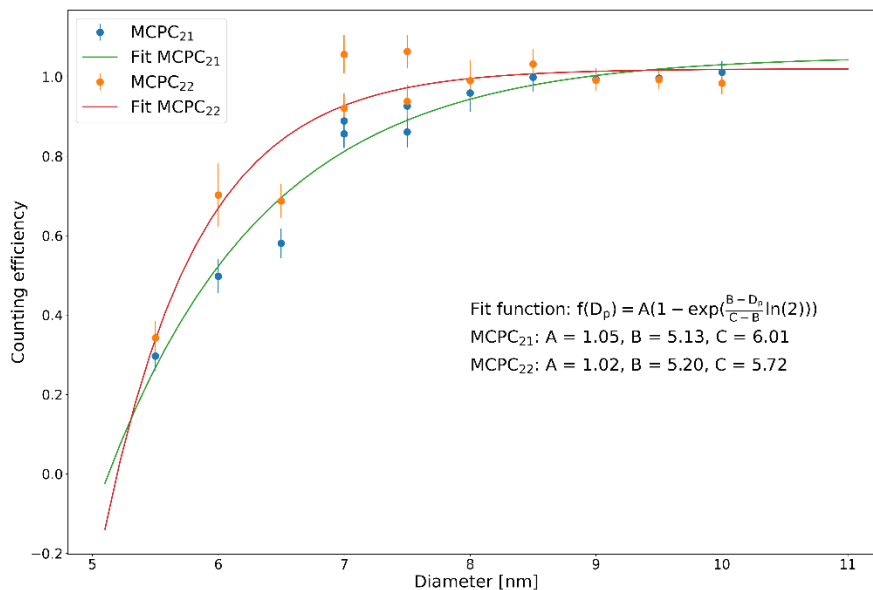
The  $d_{50}$  cutoff of both aMCPCs was tested experimentally by comparing measured concentration of the aMCPCs and a reference ultrafine CPC (CPC3022A, TSI). Particles were generated from pure MiliQ water using a portable aerosol generation system

(PAGS, Handix scientific, USA). Particles were size selected through a DMA. The two aMCPCs and reference ultrafine CPC were then connected in parallel behind the DMA. Results are shown on Fig. S2. The experimental results were fitted with an exponential function (Eq. 2):

35

$$f(D_p) = A\left\{1 - \exp\left(\frac{B-D_p}{C-B}\ln(2)\right)\right\} \quad (2)$$

With fit results  $A = 1.05$ ,  $B = 5.13$  and  $C = 6.01$  for aMCPC21 and  $A = 1.02$ ,  $B = 5.20$  and  $C = 5.72$  for aMCPC22.



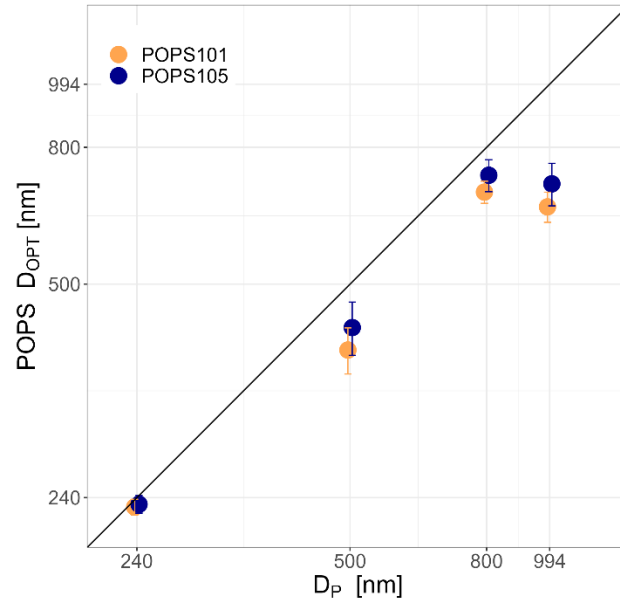
40 **Figure S2. Counting efficiency for aMCPC 21 and 22. The fitting function indicates a  $d_{50}$  cutoff of 6 nm for aMCPC 21 and 5.7 nm for aMCPC 22.**

## S.2 POPS (Printed Optical Particle Spectrometer) Sizing and counting efficiency characterization details

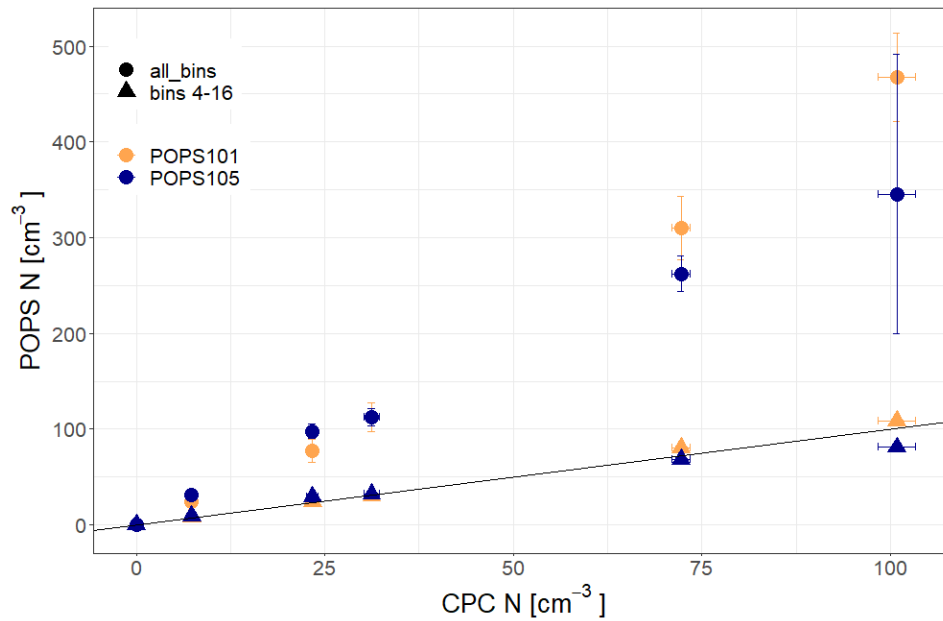
45 Sizing calibration of two POPS (1 for flights [POPS105] and 1 for ground measurements [POPS101]) were performed with polystyrene latex spheres (PSL) of sizes 240, 500, 800 and 994 nm. Nebulized particles passed inside a silica gel dryer to remove water and size selection was refined with a differential mobility analyzer (DMA). Both POPS were set to 200 bins to improve the resolution of the size distribution around the main particle size mode. For each PSL diameter, the POPS measured for 5 minutes once the concentration became stable. Figure S3 shows results from measured optical diameters ( $D_{OPT}$ ) calculated from lognormal fits of averaged PSDs. The uncertainty (error bars) is represented by one standard deviation of the fitted function. POPS105 shows deviations below 10% for PSLs up to 800 nm while POPS101 show slightly higher deviations up to 20% for 500 nm particles. Both POPS show higher deviation for 994 nm particles, i.e. 34 and 29% for POPS101 and 105, respectively. The higher deviation for particles around 1  $\mu\text{m}$  can be explained by Mie resonance in this size range and has also been observed by Pilz et al. (2022). We follow therefore their recommendations by setting the POPS size resolution to 16 bins to minimize sizing errors.

55 Counting efficiency of the two POPS was tested against a reference Mixing Condensation Particle Counter (MCPC model 1720, Brechtel Manufacturing Inc) with 230 nm PSLs. Background noise of the POPS was tested with particle-free air. Both POPS and the reference CPC showed concentration of  $0 \text{ cm}^{-3}$ . PSLs were then nebulized into the inlet. Concentrations were incrementally increased by modifying the particle-to-air ratio of the nebulizer. Figure S4 shows results of particle number concentrations of the two POPS against the reference CPC including all 16 bins (142 – 3366 nm, dots) and bins 4 to 16 (186 – 3366 nm, triangles). Bins

60 1 to 3 show increasing noise levels with higher particle concentration. These results are consistent with precedent findings (Gao et al., 2016; Mei et al., 2020; Pilz et al., 2022).



65 **Figure S3.** Measured optical particle diameter ( $D_{OPT}$ ) by two POPS determined by lognormal fits of the measured particle size distribution (PSD) of PSL particles with a given mobility diameter ( $D_P$ ). The black line represents the 1:1 line.



70 **Figure S4.** Particle number concentration of two POPS against a reference CPC. Dots represent mean concentration including all bins and triangles represent recalculated mean concentrations excluding bins 1 to 3.

### S.3 Element analysis

#### 75 S.3.1 Microwave assisted digestion of aerosol filters

For each regular filter blank, field blank and aerosol sample, half of the filter was cut with stainless steel scissors and placed into a polytetrafluoroethylene (PTFE) microwave vessel. 1 mL of nitric acid (69% HNO<sub>3</sub>, Suprapur; Roth) 1 mL of hydrogen peroxide (30% H<sub>2</sub>O<sub>2</sub>, for ultratrace analysis; Sigma-Aldrich), and 1 mL of ultrapure water (18.2 MΩ cm; Nanopure DIAMOND™ system) were then added to the PTFE microwave vessel. The digestion was performed immediately with an MLS GmbH UltraCLAVE 4 microwave using the following program: temperature ramp from 25 to 230°C over 25 min (Power, 2500W; P, 130 Bar) and then, 20 min at 230°C (Power, 2500W; P, 130 Bar). After digestion, the 6 mL sample digests were poured into 15 mL polypropylene vials, and 3 mL of ultrapure water was used to recover the remaining sample digest in the digestion vessel, which was then added to the 6 mL sample digest. The digests were then filtered at 0.45 μm (syringe filter Perfect-Flow®, Nylonmembran; BGB Analytix) and stored in the dark at 4°C until analysis. In addition to regular filter blank and field blanks, 3 procedural blanks, i.e., reagent blanks that consist of the digestion reagents subjected to the same digestion, filtration and storage procedures as the samples and filter blanks were performed. To ensure low element background in the digest, the PTFE microwave vessels were extensively cleaned before digestion of the regular filter blanks, field blanks and aerosol samples. The PTFE microwave vessels cleaning consisted of: 1) soaking them in 20 % HNO<sub>3</sub> (from 69% HNO<sub>3</sub>, ISO; Roth) overnight; 2) rinsing them three time with ultrapure water; 3) soaking them in 20% HCl (from 35% HCl, ISO; Roth) overnight; 4) rinsing them three time with ultrapure water; 5) soaking them in 20 % HNO<sub>3</sub> (from 69% HNO<sub>3</sub>, ISO; Roth) overnight; 6) rinsing them three time with ultrapure water; and 7) performing a digestion run with the vessels filled up with 3 mL of ultrapure water and 3 mL of HNO<sub>3</sub> (69%, Suprapur; Roth) using the same microwave program than for the sample digestion.

### 95 S.3.2 Quantification of elements by ICP-MS/MS

Elements were quantified in the digests using an Agilent 8900 ICP-MS/MS equipped with an SPS4 autosampler, a high-throughput injection system (ISIS) with a PTFE sample loop, a concentric nebulizer, a Scott double-pass spray chamber cooled to 2°C, a 2.5 mm i.d. quartz torch, and platinum sampler and skimmer cones. All ICP-MS/MS parameters were optimized before analysis using a tuning solution containing 10 μg L<sup>-1</sup> of lithium (Li), yttrium (Y), cobalt (Co), cerium (Ce), and tellurium (Te) (prepared with standards from J.T. Baker). Employed acquisition parameters, i.e., collision/reaction cell gas(es), single versus tandem MS mode, acquired mass to charge ratio (*m/z*), acquisition time and number of analytical replicates are given for each analyzed elements in Table S1. Quantification was done by external calibration with elemental standards (purchased at J.T. Baker) prepared in the sample digest matrix (i.e., 11% HNO<sub>3</sub> Suprapur). An internal standard containing scandium (Sc, 70 μg L<sup>-1</sup>), indium (In, 7 μg L<sup>-1</sup>) and lutetium (Lu, 7 μg L<sup>-1</sup>) was used during the analysis to check signal stability during the runs. ICP-MS/MS data-treatment was done using Agilent Masshunter software (version 4.6).

**Table S1.** ICP-MS/MS acquisition parameters for analyzed elements

Elements	ICP-MS/MS mode	Acquired <i>m/z</i>	Acquisition time (s)	Replicates number
Sodium (Na)		23	0.01	
Magnesium (Mg)		24	0.01	
Aluminum (Al)		27	0.01	
Potassium (K)	Single quadrupole mode – C/RC: 5 mL min <sup>-1</sup> He	39	0.01	3
Calcium (Ca)		43	0.01	
Vanadium (V)		51	0.1	
Iron (Fe)		56	0.05	
Zinc (Zn)		66	0.1	
Chromium (Cr)		52->52	0.1	
Manganese (Mn)	Tandem MS mode – C/RC: 5 mL min <sup>-1</sup> H <sub>2</sub>	55->55	0.1	3
Cobalt (Co)		59->59	0.1	
Nickel (Ni)		60->60	0.1	

Copper (Cu)		63->63	0.1	
Arsenic (As)		75->75	0.3	
Selenium (Se)		78->78	0.3	
Rubidium (Rb)		85->85	0.1	
Molybdenum (Mo)		98->98	0.1	
Silver (Ag)		107->107	0.1	
Cadmium (Cd)		111->111	0.1	
Lead (Pb)		208->208	0.1	
Phosphorus (P)	Tandem MS mode –	31->47	0.05	
Sulfur (S)	C/RC: 30% O <sub>2</sub> + 1 mL min <sup>-1</sup> H <sub>2</sub>	32->48	0.05	3

**Table S2: Background levels of blank filters and detection limits of analyzed elements**

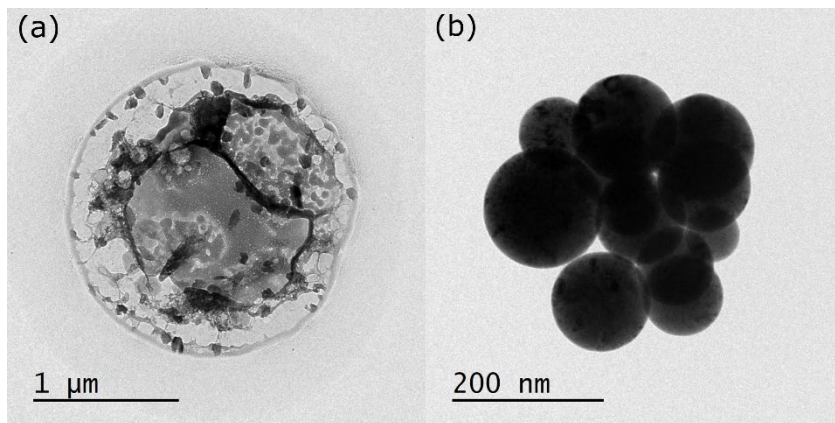
Element	Unit	Mean of background	Standard deviation of background	Detection limit
Aluminum (Al)		4	4	16
Calcium (Ca)		0.16	0.09	0.43
Chromium (Cr)		0.08	0.03	0.16
Iron (Fe)		1.2	0.2	1.9
Magnesium (Mg)		0.24	0.06	0.43
Nickel (Ni)	μg	0.08	0.02	0.15
Phosphorus (P)		0.18	0.07	0.39
Potassium (K)		0.05	0.03	0.15
Sodium (Na)		0.18	0.09	0.43
Sulfur (S)		1.1	0.3	2.0
Zinc (Zn)		0.8	0.3	1.8
Arsenic (As)		0.7	0.2	1.3
Cadmium (Cd)		0.4	0.3	1.3
Cobalt (Co)		0.9	0.4	2.0
Copper (Cu)		8	5	22
Lead (Pb)		9	4	22
Manganese (Mn)	ng	16	5	30
Molybdenum (Mo)		17	3	25
Rubidium (Rb)		0.8	0.8	3.2
Selenium (Se)		0.05	0.02	0.12
Silver (Ag)		0.12	0.06	0.30
Vanadium (V)		0.9	0.7	3.1

110

#### S.4 Transmission electron microscopy (TEM)

Example of particles collected during airborne sampling on September 28, 2021. Particle (a) presents a heterogeneous composition of an internally mixed particle with a denser core surrounded by lighter elements, as indicated by the brighter shading and a spherical shape. Particle (b) is an agglomerate of more homogeneous particles, likely composed of soot.

115



120

**Figure S5: TEM images of two particles collected during airborne sampling on September 28. The images are acquired under bright field imaging conditions at an accelerating voltage of 120 kV.**